Journal of the Korean Institute of Illuminating and Electrical Installation Engineers (2011) 25(3) : 50~64
DOI : 10.5207/JIEIE.2011.25.3.050

Power control strategies of a DC-coupled hybrid power system for a building microgrid

Jea-Hoon Cho* · Won-Pyo Hong**

Abstract

Abstract - In this paper, a DC-coupled photovoltaic (PV), fuel cell (FC) and ultracapacitor hybrid power system is studied for building microgrid. In this proposed system, the PV system provides electric energy to the electrolyzer to produce hydrogen for future use and transfer to the load side, if possible. Whenever the PV system cannot completely meet load demands, the FC system provides power to meet the remaining load. The main weak point of the FC system is slow dynamics, because the power slope is limited to prevent fuel starvation problems, improve performance and increase lifetime. A power management and control algorithm is proposed for the hybrid power system by taking into account the characteristics of each power source. The main works of this paper are hybridization of alternate energy sources with FC systems using long and short storage strategies to build an autonomous system with pragmatic design, and a dynamic model proposed for a PV/FC/UC bank hybrid power generation system. A simulation model for the hybrid power system has been developed using Matlab/Simulink, SimPowerSystems and Matlab/Stateflow. The system performance under the different scenarios has been verified by carrying out simulation studies using a practical load demand profile, hybrid power management and control, and real weather data.

Key Words : Photovoltaic (PV), Fuel Cell (FC), Ultracapacitor bank, DC-Coupled Hybrid Power System, Matlab/Simulink and SimPowerSystems, Matlab/Stateflow

1. Introduction

The ever increasing energy consumption, the soaring cost and the exhaustible nature of fossil fuel, and the worsening global environmental issues present renewable energy sources as promising solutions. Wind turbines, solar energy and fuel cells have experienced a remarkably rapid growth in the past ten years because they are pollution-free sources of power. Recent advancement in

* Main author : Dept. of Electrical & Computer Engineering, Chungbuk National University, Korea
** Corresponding author : Dept. of Building Services Engineering, Hanbat National University, Korea
Tel : +82-42-821-1179, Fax : +82-42-821-1175
E-mail : wphong@hanbat.ac.kr
Date of submit : 2011. 2. 28
First assessment : 2011. 3. 5
Completion of assessment : 2011. 3. 16

hydrogen-powered applications makes an indispensable energy carrier for the hydrogen economy. In particular, PEM fuel cells seem to be a good option to be implemented as a distributed generation (DG) in the distribution system of building microgrid.

Fuel cell-based distributed generation has been receiving more attention in the last year because of its high efficiency, low aggression to the environment, no moving parts and superior reliability, durability, and the rapid progress in FC technology. However, each of the aforementioned technologies has its own drawbacks. Different energy sources and converters need to be integrated to meet sustained load demands while accommodating various natural conditions. In future energy systems, renewable energy sources will be used to generate hydrogen, and power demand might be satisfied using renewable sources and fuel cells in hybrid topologies since the hydrogen economy is one vision of the future. Therefore, distributed energy resources such as PV cells and wind turbines can be co-operated with fuel cells, various stand-alone systems, and grid-connected systems. The power generated by a PV system is highly dependent on weather conditions. For example, during cloudy periods and at night, a PV system would not generate any power. In addition, it is difficult to store the power generated by a PV system for future use. To overcome this problem, a PV system can be integrated with other alternate power sources and/or storage systems, such as electrolyzers, hydrogen storage tanks, FC systems or UC banks [1-3]. The combination of an FC system and UC bank is an attractive choice due to their high efficiency, fast load response, and flexible and modular structure for use with other alternative sources such as PV systems or wind turbines.

Fuel cells (FC) basically convert the chemical energy of hydrocarbon fuels, typically hydrogen directly into dc form of electrical energy. The commonly available FCs include polymer membrane, alkaline, phosphoric acid, molten carbonate, and solid oxide-based FCs [4].

The main reasons for rushing the FC technology toward commercialization include fuel availability, modularity and cleanness of FC-based power generation. FCs are capable of generating both electrical and thermal energy. Among the various types of FCs, proton exchange membrane FCs (PEMFCs) are particularly attractive for residential use due to their relatively low operating temperature (80[℃]) and good dynamic response [5]. An FC-based power system mainly consists of a fuel-processing unit (reformer), FC stack and power conditioning unit.

An FC power plant uses oxygen and hydrogen to convert chemical energy into electrical energy. Due to the low working temperature and fast start up, PEM fuel cell power plants (FCPPs) are one of the promising candidates for residential and commercial applications [5]. In this study, a PEMFC power plant is preferred because, among the various types of FC systems, PEMFC power plants have been found to be especially suitable for hybrid power systems [3]. However, the FC system has a weak point of slow dynamics because the power slope is limited to prevent fuel starvation problems, improve performance and increase lifetime. The very fast power response and high specific power of an ultracapacitor complements the slow power output of an FC system. Recent progress in technology makes ultracapacitors the best candidates of fast dynamic energy storage devices, especially for smoothing fluctuant energy production in hybrid power systems. Compared to batteries, ultracapacitors are capable of very fast charges and discharges with high power density and can achieve

a very large number of cycles without degradation, even at 100[%] depth of discharge without "memory effect." Globally, super-capacitors have a better round-trip efficiency than batteries [6]. Without the UC bank, the FC system must supply all power demands, thus increasing the size and cost of the FC power plant. Besides, overloading of fuel cell systems may cause gas starvation, thus decreasing its performance and lifetime.

In Ref. [7], a detailed dynamic model, design and simulation of a wind/FC/UC-based hybrid power generation system is described. The paper of Alam [8] used a simplified model of a DC-DC converter, inverter, power controller and MPPT algorithm for simulating a hybrid power system. In this paper, DC-coupled photovoltaic (PV), fuel cell (FC) and ultracapacitor hybrid power systems are studied for building microgrid. A power management and control algorithm is proposed for the hybrid power system by taking into account the characteristics of each power source. The main works of this paper are hybridization of alternate energy sources with FC systems using long and short storage strategies to build an autonomous system with pragmatic design, and a dynamic model proposed for a PV/FC/UC bank hybrid power system. A simulation model for the hybrid power system has been developed using Matlab/Simulink, SimPowerSystems and Matlab/Stateflow. The system performance under the different scenarios has been verified by carrying out simulation studies using a practical load demand profile, hybrid power management and control, and real weather data of the Deajeon area. Model parameters are referred to in [8] because of a deficiency of verified data in Korea. Dynamic Modeling and simulations are performed using MATLAB/Simulink and SimPowerSystems [9] packages, and the results are presented to verify the effectiveness of the proposed system under peak power demands or transient conditions. In particular, the detailed power converter controllers developed and turned to be reduced power fluctuations. The Matlab/Stateflow chart of incremental conductance algorithms for a direct control method is applied for MPPT of PVs for the first time.

2. System descriptions in hybrid power systems

2.1 System configuration

A very possible stand-alone solar cell - hydrogen hybrid power system consists of a PV panel with maximum power point trackers (MPPT) for solar energy conversion, a pressurized advanced alkaline electrolyzer with a DC/DC converter for H_2 production, a pressurized tank for seasonal H_2 storage, fuel cells with a DC-DC converter for H_2 utilization, a ultracapacitor bank for a short-time electricity energy buffer, and a DC/AC inverter for the user load [10-11]. A PV panel converts solar irradiations into electricity. For the increase of overall system efficiency, the DC/DC converter with MPPT enables the PV panel to work at the maximum power point in a highly fluctuated environment. The conversion efficiency of most prevalent silicon solar cells is approximately 10-30[%] at ambient temperature 25[°] [12]. Here, to sustain the power demand and solve the energy storage problem, electrical energy can be stored in the form of hydrogen. By using an electrolyzer, hydrogen can be generated and stored for future use.

The hydrogen produced by the electrolyzer using PV power is used in the FC system and acts as an energy buffer. Thus, the effects of reduction and even the absence of the available power from the PV system can easily be tackled. In the integrated

system, the necessary measurements are performed, and measurement results are conveyed to the main controller. The main controller evaluates the inputted data and takes the required actions to provide the overall controls. Here, each shown dc/dc converter consists of two cascade dc/dc converters; one for the power tracking and the other for bus voltage regulation. The primary objective of such a solar-hydrogen system is to provide sufficient and reliable electricity to meet the end-use power demand and store the excess energy in the ultracapacitor and hydrogen. For a sustainable stand-alone solar-hydrogen system, all the energy required by user load comes from the solar irradiation via the PV panel. Excluding the partial solar power for meeting a certain load demand, the excess solar power will eventually be stored in both a super capacitor and an H_2 tank. In practice, the energy capacity of the H_2 tank is usually much higher than that of the battery. Therefore, the final amount of H_2 in the storage tank is the key performance index for energy efficiency [13], i.e. the larger the amount of H_2 in the storage tank, the higher the energy efficiency. The energy efficiency is significantly determined by the energy management strategy for the stand-alone solar-hydrogen systems. Fig. 1 shows the integrated overall layout of the Simulink model. This figure comprises the PV, ultracapacitor bank and PEMFC system. To control and manage its integration system, the power management, power estimator and controller block are provided.

2.2 PV system characteristics and model

To sustain its continuous operation, the stand-alone solar—hydrogen system must at least maintain energy balance over several years. A PV system consists of many cells connected in a series and parallel to provide the desired output voltage. Usually, the PV system exhibits a nonlinear I-V characteristic [14, 15], and the PV equations for modeling the characteristic have been developed. A verified model for a silicon solar PV panel is introduced in [14]. Recently, the detailed models,

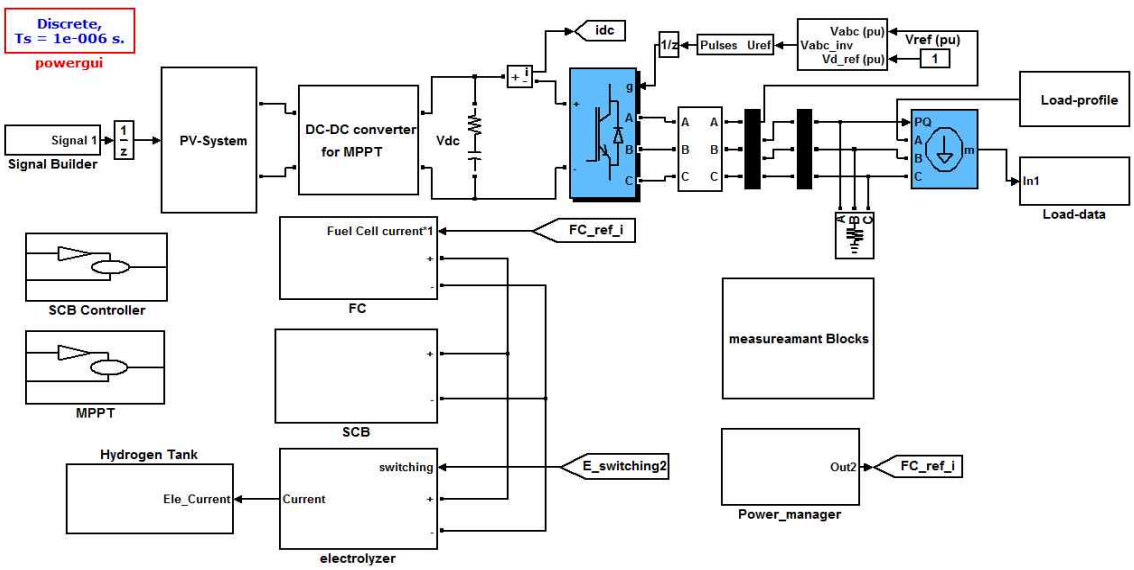

Fig. 1. Overall layout of the Matlab/Simulink model

including nonlinear effects such as resistive losses, non-ohmic-current and temperature, have been developed for a more accurate model. In this paper, a simple equation model, which represents the dynamic nonlinear I-V characteristics of the PV system, is modified and can be used for analyzing the effects among components of the hybrid system. The parameters used in the mathematical modeling of the PV cells are as follows:

a	ideality or completion factor
I_0	PV cell reverse saturation current [A])
I_{PV}	PV cell output current [A]
I_{sc}	short-circuit cell current (representing insolation level [A])
k	Boltzmann's constant [J/_K]
N_p	the number of parallel strings
N_s	the number of series cells per string
q	electron charge [C]
R_s	series resistance of PV cell [U]
T	PV cell temperature [_K]
V_{OC}	open-circuit voltage [V]
V_{PV}	terminal voltage for PV cell [V]

The output voltage characteristic of the PV system may be expressed as [18, 19]:

$$V_{PV} = \frac{N_s \alpha k T}{q} \ln\left[\frac{I_{sc} - I_{PV} + N_p}{N_p I_0}\right] - \frac{N_s}{N_p} R_s I_{PV} \qquad (1)$$

The manufacturer's datasheet provides necessary information for most of the parameters of Eq. (1) [16]. The current-voltage characteristics of the PV array can be obtained and analyzed by using Eq. (1). Using the current-voltage curves, the current-power curves can be obtained to operate with maximum efficiency and produce the maximum power output. The maximum power output of the PV array varies according to solar radiation or temperature. Therefore, a maximum power point tracker (MPPT) is needed to maintain the solar array more effectively as an electric power source [17, 18]. Fig. 2 shows the PV system model with dc-dc converter designed by Matlab/SimPowerSystems.

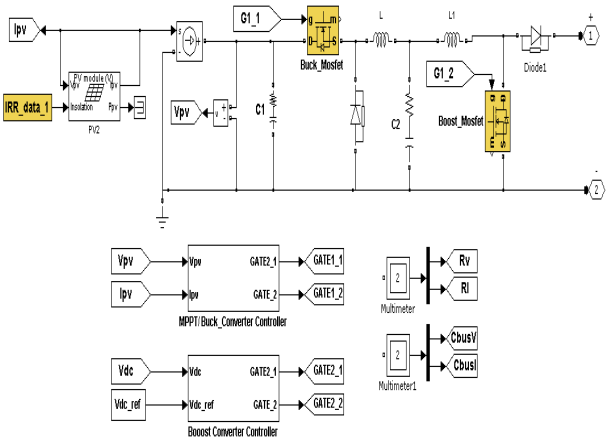

Fig. 2. PV system model with DC-DC converter

The perturb and observe (P&Q) algorithm, also known as the "hill climbing" method, is very popular and the most commonly used in practice because of its simplicity.

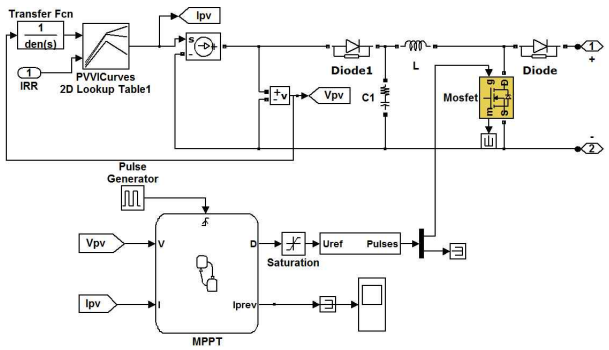

Fig. 3. The direct control model of PV system with dc-dc converter

However, there are some limitations, such as the fact that it cannot determine when it has actually reached the MPP and oscillates the operating around

the MPP. Thus, the modified algorithms for solving this problem have been studied recently.

Among different MPPT algorithms, the Incremental Conductance (IncCond) method, which can solve the problem of the P&Q algorithm, is used in this paper. For evaluating the performance of the whole system under the Matlab simulation environment, the IncCond method is developed by the Matlab/Stateflow tool. The IncCond method adjusts the PV operating point with small steps and uses an average value of 100 samples to avoid oscillation around the MPP.

In this paper, the direct control of the MPPT algorithm is adopted for changing the duty cycle of a dc-dc converter. A PI controller can be used in general MPPT algorithms, but requires a control loop for regulating the current of MPP calculated by the MPPT algorithm. Compared with the general MPPT algorithms, the direct control of the MPPT algorithm shown in Fig. 3 is simpler and uses only one control loop, in which the PI controller is excepted because it performs the adjustment of duty cycle within the MPPT algorithm.

2.4 Design and dynamic model of a PEMFC

An enhanced version of the PEMFC model described in Refs. [8, 19] is used in this study. This model is built by utilizing the relationship between the output voltage and partial pressure of hydrogen, oxygen and water. It shows the PEMFC model, which is then embedded into the SimPowerSystems of MATLAB as a controlled voltage source and integrated into the overall system. The FC system model parameters used in this model are as follows:

B,C constants to simulate the activation over voltage in *PEMFC* system [A^{-1}] and [V]

E Nernst instantaneous voltage [V]

E_0 standard no load voltage [V]

F Faraday's constant [C/kmol]

I_{FC} FC system current [A]

K_{an} anode valve constant $\frac{1}{2}$

K_{H2} hydrogen valve molar constant [kmol/(atm s)]

K_{H2O} water valve molar constant [kmol/(atm s)]

K_{O2} oxygen valve molar constant [kmol/(atm s)]

K_r modeling constant [kmol/(s A)]

M_{H2} molar mass of hydrogen [kg kmol_1]

N_0 number of series fuel cells in the stack

N_S number of stacks used in the FC power plant

p_{H2} hydrogen partial pressure [atm]

p_{H2O} water partial pressure [atm]

p_{O2} oxygen partial pressure [atm]

q_{O2} input molar flow of oxygen [kmol/s]

q_{H2} input molar flow of hydrogen [kmol/s]

$q_{H_2}^{in}$ hydrogen input flow [kmol/s]

$q_{H_2}^{out}$ hydrogen output flow [kmol/s]

$q_{H_2}^{r}$ hydrogen flow that reacts [kmol/s]

$q_{H_2}^{req}$ amount of hydrogen flow required to meet the load change [kmol/s]

R universal (Rydberg) gas constant [J/(kmol K)]

γ_{H-O} the hydrogen-oxygen flow ratio

R^{int} FC internal resistance [U]

T absolute temperature [K]

U utilization rate

V_{an} volume of the anode [m3]

V_{cell} dc output voltage of FC system [V]

τ_{H2} hydrogen time constant [s]

τ_{O2} oxygen time constant [s]

τ_{H2O} water time constant [s]

η_{act} activation over voltage [V]

η_{ohmic} ohmic over voltage [V]

The relationship between the molar flow of any gas (hydrogen) through the valve and its partial pressure inside the channel can be expressed as [19].

$$\frac{q_{H_2}}{p_{H_2}} = \frac{K_{an}}{\sqrt{M_{H_2}}} = K_{H_2} \tag{2}$$

For hydrogen molar flow, there are three significant factors: hydrogen input flow, hydrogen output flow and hydrogen flow during the reaction [20]. The relationship among these factors can be expressed as

$$\frac{d}{dt} p_{H_2} = \frac{RT}{V_{an}} (q_{H_2}^{in} - q_{H_2}^{out} - q_{H_2}^{r}) \tag{3}$$

According to the basic electrochemical relationship between the hydrogen flow and the FC system current, the flow rate of reacted hydrogen is given by [21]

$$q_{H_2}^{r} = \frac{N_0 N_s I_{FC}}{2F} = 2K_r I_{FC} \tag{4}$$

Using Eqs. (2) and (4), and applying Laplace transform, the hydrogen partial pressure can be obtained in the s domain as [21]

$$p_{H_2} = \frac{1/K_{H_2}}{1+\tau_{H_2} s} (q_{H_2}^{in} - 2K_r I_{FC}) \tag{5}$$

Where

$$\tau_{H_2} = \frac{V_{an}}{K_{H_2} RT} \tag{6}$$

Similarly, water partial pressure and oxygen partial pressure can be obtained. The polarization curve for the PEMFC is obtained from the sum of the Nernst's voltage, the activation over voltage, and the Ohmic over voltage. Assuming constant temperature and oxygen concentration, the FC output voltage may be expressed as [20, 21]

$$V_{cell} = E + \eta_{act} + \eta_{ohmic} \tag{7}$$

Where

$$\eta_{act} = -B \ln(CI_{FC}) \tag{8}$$

And,

$$\eta_{ohmic} = -R^{\text{int}} I_{FC} \tag{9}$$

Now, the Nernst's instantaneous voltage may be expressed as [21]

$$E = N_0 \left[E_0 + \frac{RT}{2F} \log \left[\frac{p_{H_2} \sqrt{p_{O_2}}}{p_{H_2O}} \right] \right] \tag{10}$$

The FC system consumes hydrogen according to the power demand. The hydrogen is obtained from the on-board high-pressure hydrogen tanks. During operational conditions, to control the hydrogen flow rate according to the output power of the FC system, a feedback control strategy is utilized. To achieve this feedback control, FC current from the output is taken back to the input while converting the hydrogen into molar form [22]. The amount of hydrogen available from the hydrogen tank is given by

$$q_{H_2}^{req} = \frac{N_0 N_s I_{FC}}{2FU} \tag{11}$$

Depending on the FC system configuration,

and the flow of hydrogen and oxygen, the FC system produces the dc output voltage. The hydrogen-oxygen flow ratio Y_{H-O} in the FC system determines the oxygen flow rate [23].

The FC system consumes hydrogen according to the power demand, where hydrogen is obtained from the storage tank. To control the hydrogen flow rate according to the FC power output, a feedback control strategy is utilized by taking output FC current back to the input.

2.4 Ultracapacitor bank (UCB) model

The ultracapacitor is an energy storage device that is able to handle fast fluctuations in energy levels. When comparing ultracapacitors with batteries, they have a significantly lower energy density than the batteries, but they have a higher power density compared to batteries [24]. For practical applications, the terminal voltage determines the number of capacitors which must be connected in series to form a bank, and the total capacitance determines the number of capacitors which must be connected parallel to the bank. The detailed model including various characteristics of an ultracapacitor can be used in modeling ultracapacitors. But, for the simplicity of simulation, a simplified equivalent model that is only used for principle verification has been used in many papers. Fig. 4 shows the simplified UC model a with bidirectional dc-dc converter.

The parameters used in the mathematical modeling of the UC bank are as follows [25]:

C	capacitance [F]
$C_{UC-total}$	the total UC system capacitance [F]
ESR, R	equivalent series internal resistance [U]
E_{UC}	the amount of energy released or captured by the UC bank[W/s]
n_s	the number of capacitors connected in series
n_p	the number of series strings in parallel
$R_{UC-total}$	the total UC system resistance [U]
V_i	the initial voltage before discharging starts [V]
V_f	the final voltage after discharging ends [V]

The amount of energy drawn from the UC bank is directly proportional to the capacitance and the change in the terminal voltage, given by

$$E_{UC} = \frac{1}{2} C \left(V_i^2 - V_f^2 \right) \tag{12}$$

The total resistance and the total capacitance of the UC bank may be calculated as

$$R_{UC-total} = n_s \frac{ESR}{n_p} \tag{13}$$

$$C_{UC-total} = n_p \frac{C}{n_s} \tag{14}$$

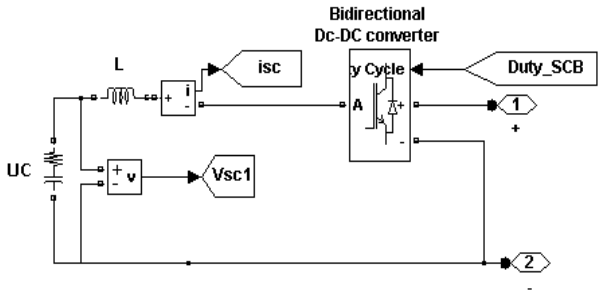

Fig. 4. The simplified UC model with bidirectional dc-dc converter

2.6. Electrolyzer model

To provide fuel cells with hydrogen, water can be decomposed into its elementary components by an

electrolyzer [26, 27]. The electrolyzer model can be described by the electrochemical reaction of water electrolysis.

$$H_2O_{(liquid)} + \text{electrical energy} \rightarrow H_{2(gas)} + (1/2)O_{2(gas)} \quad (15)$$

Usually, the simple electrolyzer model can be used for the hybrid system including various components and represented by

$$n_{H_2} = \frac{\eta_F n_c i_e}{2F} \quad (16)$$

$$\eta_F = 96.5e^{(0.09/i_e - 75.5/i_e^2)} \quad (17)$$

F Faraday constant [I/kmol]
i_e electrolyzer current [A]
n_c the number of electrolyzer cells in series
η_F Faraday efficiency
η_{H2} produced hydrogen moles per second [mol/s]

According to Eqs. (16) and (17), a simple electrolyzer model is developed using Matlab/ Simulink, which is illustrated in Fig. 5.

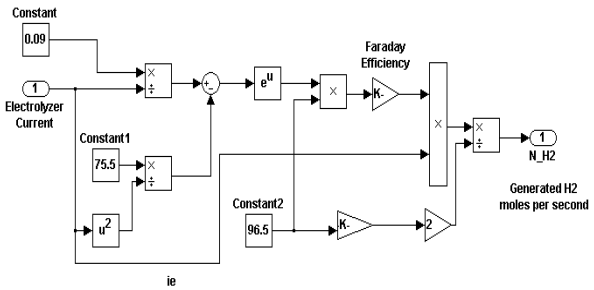

Fig. 5. The Matlab/Simulink diagram of the electrolyzer model

2.7 Hydrogen tank model

The hydrogen produced by an electrolyzer provides hydrogen to the FC system. The remaining hydrogen is sent to a storage tank. The increase and decrease of tank pressure relates to the amount of hydrogen produced by the electrolyzer and the amount of hydrogen consumed by the FC system. The parameters used in the hydrogen tank model are listed below:

M_{H_2} Molar mass of hydrogen [kg kmol^{-1}]
N_{H_2} Hydrogen moles per second delivered to the storage tank[kmol/s]
P_b Pressure of tank[Pascal]
P_{bi} Iitial pressure of the storage tank[Pascal]
R Universal(Rydberg) gas constant[J/(kmol K)]
T_b Operating temperature [°K]
V_b Volume of the tank[m^3]
z Compressibility factor as a function of pressure

The hydrogen tank model can be expressed as follows

$$P_b - P_{bi} = z\frac{N_{H_2} R T_b}{M_{H_2} V_b} \quad (18)$$

2.8 Hybrid power control strategy

In this section, a control strategy is described for the simulation of the hybrid system integrated by using each component. In a power system, power converters introduce some control inputs for the power conversion. In this case, the structure of the control system can be divided into different levels as shown in Fig. 6. The main behavior of the control strategy is to control power flow in order to meet the demand power. A main controller is employed for the entire energy measurement and management process. The power limitation of the FC is 5[kW],

and the PV system is capable of delivering 12[kW] of power at best radiation conditions (1000[W/m^2]). The UC power is limited by the maximum current of 750[A] as recommended by the manufacturer. For high efficiency of the hybrid system, the UCB needs to provide insufficient power to a load. The operating strategies used in the main controller are as follows:

- The use of power generated by the PV system has priority in satisfying power demand over that provided by the FC system or by the UC bank.
- If the total power generated by the PV system is higher than the demand, the additional power will be used to charge the UC bank.
- After charging the UC bank, the remaining power is sent to the electrolyzer through a power converter to generate hydrogen.
- The electrolyzer is kept in operation as long as available power exists and the tank pressure does not exceed the prescribed value of 15,000 Pascal. The electrolyzer's maximum power is also set to 10[kW]. The additional power generated by the PV system can be transferred to the electrolyzer up to the 10[kW] limit.
- Dumping power is necessary if the UC bank is fully charged and the electrolyzer power is at the 10[kW] limit.
- If the total electric power generated by the PV system is less than the demand, power will be supplied from the FC system up to the maximum 5[kW] limit. If the load demand exceeds the power generated by the PV/FC combination, the difference is supplied by the UC bank.
- The UC bank not only provides the excess power demand over 5[kW], but also compensates the tracking mismatches and delays of the FC system, which has a relatively slow response time.
- The UC bank maximum voltage is set to be its nominal voltage of 48[V], and its minimum voltage is set to be 20[%] of its full state of charge (SOC) to avoid overcharging and deep discharging. To implement the aforementioned power management strategy, appropriate power control systems are used at relevant points and the total system components are integrated.

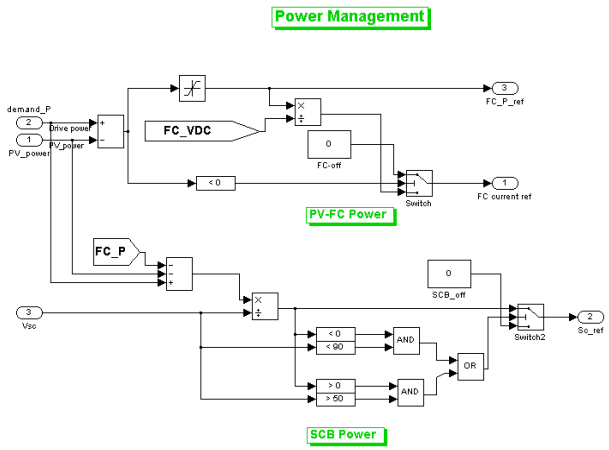

Fig. 6. The general decision algorithm used in the main hybrid power controller

3. Simulation results and analysis

The block diagram of the integrated PV/FC/UC hybrid power system and the control strategy are shown in Figs. 1 and 6, respectively. For the simulated model, the parameters of the PV system are listed in Table 1. The PEMFC system parameters are given in Table 2. The parameters of the Maxwell Boostcap BMOD0165-48.6[V] unit are used and the characteristics of the UC unit are shown in Table 3.

In order to verify the system performance under

Table 1. PV system model parameters

Parameter	Value
The number of series cells per string(N_s)	105
The number of parallel cells per strings(N_p)	148
Ideality or completion factor(a)	1.9
Boltzmann's constant(k)	1.3805e-23[J/°K]
PV cell temperature(T)	298[°K]
Electron charge(q)	1.6e-19C
Short-circuit cell current(I_{sc})	2.926[A]
PV cell reverse saturation current(I_0)	0.00005[A]
Series resistance of PV cell (R_s)	0.0277[Ω]

Table 2. PEMFC system model parameters

PEMFC Parameters	Values
Activation voltage constant (B)	0.04777[A^{-1}]
Activation voltage constant (C)	0.0136[V]
Faraday's constant (F)	96484600[C/kmol]
Hydrogen time constant(τ_{H_2})	3.37[s]
Hydrogen valve constant(K_{H_2})	4.22×10^{-5}[kmol/(atm s)]
Hydrogen-oxygen flow ratio(r_{H-O})	1.168
K_r constant = $N_0 / 4F$	2.2802×10^{-7}[kmol/(s A)]
No load voltage (E_0)	0.8[V]
Number of cells (N_0)	88
Number of stacks (N_s)	1
Oxygen time constant(τ_{O_2})	6.74[s]
Oxygen valve constant(k_{O_2})	2.11×10^{-5}[kmol/(atm s)]
FC system internal resistance(R_{int})	0.00303[Ω]
FC absolute temperature(T)	343[K]
Universal gas constant (R)	8314.47[J/(kmol K)]
Utilization factor (U)	0.8
Water time constant(τ_{H_2O})	18.418[s]
Water valve constant(K_{H_2O})	7.716×10^{-6}[kmol/(atm s)]

different situations, simulation is carried out using practical load demand data and real weather data. The simulation results are described and analyzed

Tabel 3. Ultracapacitor module parameters

UC parameters	Value
Capacitance[F]	165
Internal series resistance (dc)[mΩ]	6.1
Leakage current[A]	0.0052, 72 h, 25 C
Operating temperature	40 C to 65 C
Voltage[V]	48.6
Short-circuit current[A]	4800
Power density[W/kg]	7900
Energy density[Wh/kg]	3.81

with respect to the general behavior of each component. In the simulation process, the aim was to observe the proposed system's behavior over a long period of time including day and night cases. The load profile and solar radiation profiles are used to test the performance of the proposed hybrid system for a typical day. Power demand is obtained from typical real data to simulate a real-world scenario. Fig. 7 shows the load profiles obtained from a small building in Deajeon, where the building is approximately 3000 sq. ft. It is based on typical load demand data provided by KEPCO, an average load demand as shown in Fig. 8. The solar radiation data, which is recorded by the Korea regional meteorological station in the month of July in Daejeon city, was utilized. Using the nonlinear curve fitting based computation, the relationship between the solar radiation and the short-circuit current is obtained. We observe that in the early morning before 7:00 and in the evening after 19:00, the solar power is unavailable due to non-existence of solar radiation. The maximum power from the PV system can be transferred to the dc bus at about 12:30. As mentioned earlier, the use of power generated by the PV system has priority in satisfying load demand. Thus, the power generated by the PV system in Fig. 9 is transferred to the dc bus directly. In particular, Fig. 10 shows the current of the PV system at MPP.

This novel result is obtained from the Matlab/Stateflow chart of incremental conductance algorithms for the direct control method. The difference between the power generated PV system and the user power demand is depicted by analyzing the data. The surplus power is the additional power generated by the PV source, which is used for the UC charging and hydrogen production within the electrolyzer system. Furthermore, insufficient power is the exceeded power demands which are met by the FC system and UC bank discharge. The FC system power command is obtained according to the negative regions of the insufficient power (exceeded user demands) up to the 5[kW] limit. The power produced by the FC system is given in Fig. 11, which slightly differs from the power command due to the time constants and relatively slow response characteristic of the FC system. However, since the required hydrogen is not processed by a reformer and provided directly, the reformation time delays are eliminated. The tracking mismatch of the FC is supposed to be supplied by the UC bank. The amount of power transferred to the electrolyzer shown in Fig. 12 corresponds well to the hydrogen flow from the electrolyzer to the storage tank. Fig. 13 represents the amount of hydrogen produced by the electrolyzer. The power consumption used by the electrolyzer matches up to the hydrogen flow from the electrolyzer to the storage tank as depicted in Fig. 13. Fig. 14 illustrates the variation of pressure of the storage tank caused by the hydrogen produced by the electrolyzer and consumed by the FC. The hydrogen tank pressure increases accordingly as the electrolyzer produces hydrogen, and its pressure decreases accordingly as the FC consumes the stored hydrogen. The power supplied by the UC bank is shown in Fig. 15, which includes the exceeded load demand and the tracking mismatches of the FC system. Thus, the positive power region represents the power released by the UC bank, and the negative power region represents the power captured by the UC bank through the bi-directional dc/dc converter. Additionally, it also represents the fact that the new power management and control units are operated reliably and controller parameters are tuned accurately. Finally, Fig. 16 shows that the DC-link voltage, which requires much more sophisticated control strategies, is remarkably stable. As shown in Fig. 16, although the PV system and the FC system fluctuate due to weather conditions and load variations, the hybrid system including each component successfully keeps the dc-link voltage.

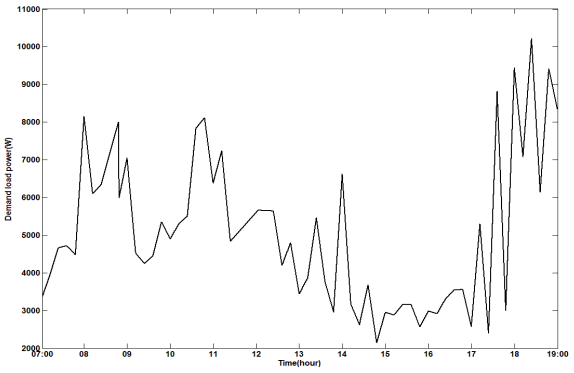

Fig. 7. Power demand of small buildings in Deajeon

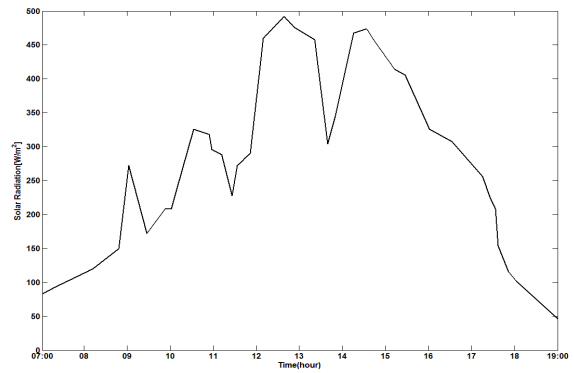

Fig. 8. Solar radiation

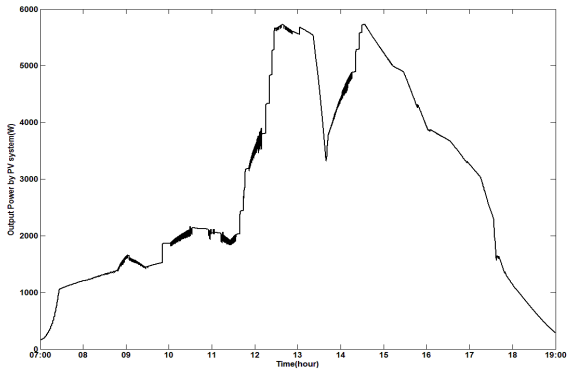

Fig. 9. Power provided by PV system

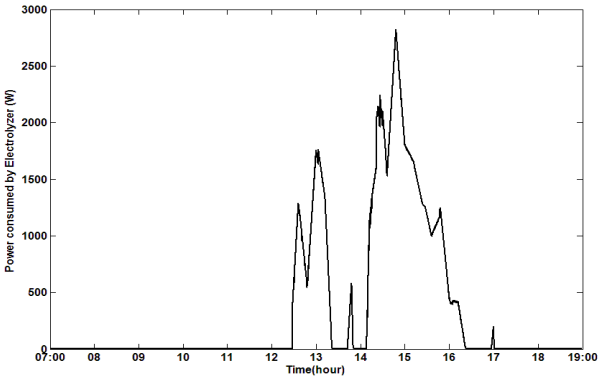

Fig. 12. Power consumed by electrolyzer

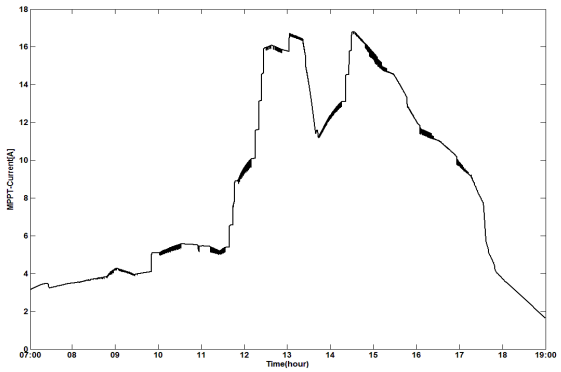

Fig. 10. Current of PV system at MPP

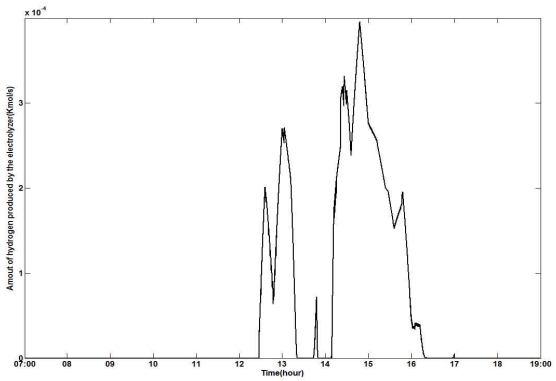

Fig. 13. Amount of hydrogen produced by the electrolyzer

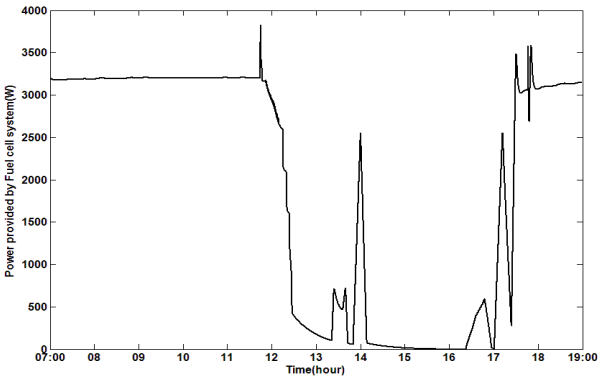

Fig. 11. Power produced by FC system

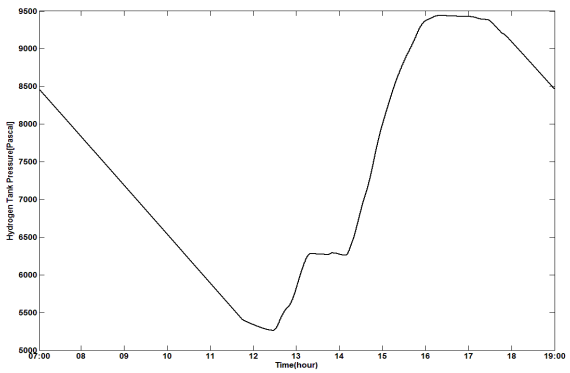

Fig. 14. The pressure variation of hydrogen tank

5. Conclusion

In this paper, a DC-coupled hybrid power system is studied with the three kinds of energy sources: (1) a photovoltaic with new MPPT methodology by the Matlab/Stateflow chart as a renewable energy

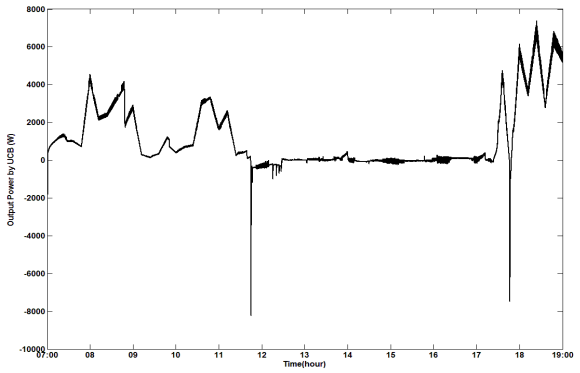

Fig. 15. Output power supplied by UCB

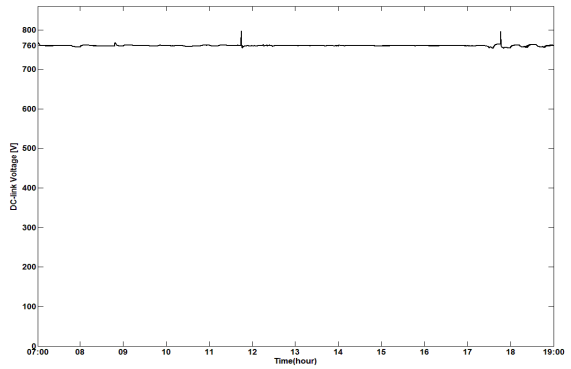

Fig. 16. DC-link voltage

generation system, (2) ultra-capacitors as fast-dynamic energy storage system, and (3) fuel cells with electrolyzers and a hydrogen tank as a long-term energy storage system. The structure of the control system is divided into three levels: (1) switching control unit, (2) automatic control unit, and (3) power management and control unit. The hybrid power system is designed and modeled for a stand-alone building microgrid use with appropriate power management controllers and power converters. The available power from the PV energy source is highly dependent on environmental conditions. To overcome this deficiency in the PV technology, we integrated the PV system with the FC/UC system using a new topology and detailed converters model.

A detailed simulation model has been developed which allows designing and analyzing any PV/FC/UC hybrid system with various power levels and parameters. The dynamic performances of the hybrid system are tested under varying solar radiation and load demand conditions where the solar radiation and power demand data are based on real records. The proposed system and its power management and control strategy exhibit excellent performance from simulation results for the simulation of a complete day or longer periods of time.

References

[1] Kyoungsoo R, Rahman S. Two-loop controller for maximizing performance of a grid-connected photovoltaic-fuel cell hybrid power plant. IEEE Transactions Energy Conversion 1998; 13(3), pp.276-281.

[2] El-Shatter TF, Eskandar MN, El-Hagry MT. Hybrid PV/fuel cell system design and simulation. Renewable Energy 2002; 27(3), pp.479-485.

[3] Gorgun H. Dynamic modeling of a proton exchange membrane (PEM) electrolyzer. International Journal of Hydrogen Energy 2006, 31(1), pp. 29-38.

[4] M. Farooque and H. C. Maru, "Fuel cells-the clean and efficient power generators," Proc. IEEE, vol. 89, no. 12, pp. 1819-1829, Dec. 2001.

[5] J. E. Larmine and A. Dicks, Fuel Cell Systems Explained. Chichester, U.K.: Wiley, 2000.

[6] Burke A. Ultracapacitors: why, how and where is the technology. Journal of Power Sources 2000; 91(1):37-50.

[7] Onar O.C, Uzunoglu M, Alam M.S. Dynamic modeling, design and simulation of a wind/fuel cell/ultra-capacitor based hybrid power generation system. Journal of Power Source 2006; 161(1):707-22.

[8] Uzunoglu M, Onar O.C, Alam M.S. Modeling, control and simulation of a PV/FC/UC based hybrid power generation system for stand-alone application. Renewable Energy; 32(2009), pp. 509-520.

[9] MATLAB SimPowerSystems for use with Simulink user's guide, version 4.1.1. Available from: <http://www.mathworks.com/access/helpdesk/help/pdf_doc/physmod/powersys/powersys.pdf>

[10] Stantarelli M, Calı' M, Macagno S. Design and analysis of stand-alone hydrogen energy systems with different renewable sources. Int J Hydrogen Energy 2004; 29:1571-1586.

[11] Barthels H, Brocke WA, Bonhoff K, et al. Phoebus-Ju¨lich: an autonomous energy supply system comprising photovoltaics, electrolytic hydrogen, fuel cell. Int J

Hydrogen Energy 1998; 23, 295-301.
[12] Klein SA, Beckman WA, Mitchell JW, et al. TRNSYS—A transient simulation program, Solar Energy Laboratory, University of Wisconsin-Madison, 2004.
[13] Ulleberg Ø. "The importance of control strategies in PV-hydrogen systems," Solar Energy 2004, 76, pp. 323-329.
[14] Masoum MAS, Dehbonei H, Fuchs EF. Theoretical and experimental analyses of photovoltaic systems with voltage and current-based maximum power-point tracking. IEEE Transactions on Energy Conversion 2002; 17(4), pp.514-522.
[15] Veerachary M, Senjyu T, Uezato K. Voltage-based maximum power point tracking control of PV system. IEEE Transactions on Aerospace and Electronic Systems 2002; 38(1):262-270.
[16] Sukamongkol Y, Chungpaibulpatana S, Ongsakul W. "A simulation model for predicting the performance of a solar photovoltaic system with alternating current loads," Renewable Energy, 2002; 27(2), pp.237-258.
[17] Chedid R, Rahman S., "A decision support technique for the design of hybrid solar-wind power systems", IEEE Transactions on Energy Conversion 1998; 13(1), pp.76-83.
[18] Kobayashi K, Matsuo H, Sekine Y., "Novel solar-cell power supply system using a multiple-input DC-DC converter," IEEE Transactions on Industrial Electronics 2006; 53(1), pp.281-186.
[19] El-Shark MY, Rahman A, Alam MS, Byrne PC, Sakla AA, Thomas T., "A dynamic model for a stand-alone PEM fuel cell power plant for residential applications," Journal of Power Sources 2004; 138(1-2), pp.199-204.
[20] Padulles J, Ault GW, McDonald JR., "An integrated SOFC plant dynamic model for power systems simulation," Journal of Power Sources 2000; 86(1-2), pp. 495-500.
[21] Gao L, Dougal RA, Liu S. Power enhancement of an actively controlled battery/ultracapacitor hybrid. IEEE Transactions on Power Electronics 2005; 20(1), pp. 236-243.
[22] Hamelin J, Agbossou K, Laperriere A, Laurencelle F, Bose TK., "Dynamic behavior of a PEM fuel cell stack for stationary applications," International Journal of Hydrogen Energy 2001; 26(6), pp.625-269.
[23] Hauer KH. "Analysis tool for fuel cell vehicle hardware and software (controls) with an application to fuel cell economy comparisons of alternative system designs," Ph.D. Dissertation, Department of Transportation Technology and Policy, University of California Davis, 2001.
[24] Johansson, P.: Comparison of Simulation programs for Supercapacitor Modeling. Chalmers University of Technology, Master of Science thesis (2008).
[25] Spyker RL, Nelms RM., "Analysis of double-layer capacitors supplying constant power loads," IEEE Transactions on the Aerospace and Electronic Systems 2000; 36(4), pp.1439-1443.
[26] Khan MJ, Iqbal MT., "Dynamic modeling and simulation of a small wind-fuel cell hybrid energy system," Renewable Energy, 2005; 46(3), pp. 421-39.
[27] Ulleberg O., "Stand-alone power systems for the future: optimal design, operation and control of solar-hydrogen energy systems," Ph.D. dissertation, Norwegian University of Science and Technology; 1998.

Biography

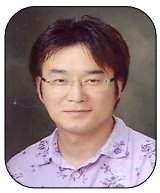

Jae-Hoon Cho

Jae-Hoon Cho received an M.S degree in Control and Instrumentation Engineering from Hanbat National University, Korea in 2002. He is working toward a Ph.D. degree in Electrical and Computer Engineering at Chungbuk National University, Korea. His interests are evolutionary computation, swarm intelligence, pattern recognition, neural network, and bioinformatics.

Won-Pyo Hong

Won-Pyo Hong was born in Daejeon city in the Republic of Korea on May 15, 1956. He received a B.S. degree in Electrical Engineering from Sungsil University, Seoul, Korea, in 1978 and M.Sc. and Ph.D. degrees in Electrical Engineering from Seoul National University, Seoul, Korea, in 1980 and 1989, respectively. From 1980 to 1993, he was senior researcher of the Korea Electric Power Research Institute at the Korea Electric Power Cooperation. He was visiting professor at the UBC, Canada, from 2007 to 2008. He is a professor in the Department of Building Services Engineering of Hanbat National University, where he has taught since 1993. His main research interests are building energy and management systems, green buildings, field bus-based control and distributed energy resources.